The surface properties of bornite

DAVID J. VAUGHAN

Department of Geological Sciences, Aston University, Birmingham B4 7ET, U.K.

JOHN A. TOSSELL

Department of Chemistry, University of Maryland, College Park, Maryland 20742, U.S.A

AND

CHRIS. J. STANLEY

Department of Mineralogy, British Museum (Natural History), Cromwell Road, London SW7 5BD, U.K.

Abstract

The surfaces of fresh and tarnished (through exposure to the atmosphere) bornite have been studied by measurement of reflectance and quantitative colour parameters in the visible region, X-ray photoelectron and Auger electron spectroscopy, and conversion electron Mössbauer spectroscopy. The results of these studies, in combination with those of previous workers, indicate that a surface coating of an iron hydroxy-oxide forms on bornite, leaving beneath it a layer with a copper sulphide composition. A model to explain this alteration process is proposed based on a suggested surface reconstruction in bornite, leading to metals in essentially trigonal planar coordination. Resulting destabilization of iron relative to copper in this crystal chemical environment is suggested to account for its preferential oxidation.

KEYWORDS: bornite, surface properties, tarnish, sulphides.

Introduction

BORNITE (Cu_5FeS_4) is an important ore mineral of copper and whereas freshly cleaned or polished surfaces have a 'bronze' colour, a tarnish appears after a short period of exposure to the atmosphere giving purple and blue colouration. Bornite is, therefore, an example of a relatively rapidly tarnishing sulphide mineral and a good subject of study in regard to the nature of such surface reactions in sulphides.

In this contribution, the physical and chemical nature of the bornite surface in relation to the bulk in the 'pure' mineral, the changes occurring during the development of a tarnish and the nature of the tarnish reaction are considered in the light of previously published work, and our new studies involving reflectance measurements, X-ray photoelectron (ESCA) and Auger electron spectroscopy, conversion electron Mössbauer spectroscopy and electron microprobe measurements.

Sample origins and compositions

Bornite specimens from the collections of the British Museum (Natural History) were used in the studies described below. Most of the work was undertaken on sample BM 31324, a massive bornite sample from Monte Catini, Tuscany, Italy. Examination of this sample in polished section and by electron microprobe analysis (Table 1) showed it to be a homogeneous sample of high purity. Another specimen, BM 1969,215, from Tsumeb, Namibia, was also analysed by electron microprobe (Table 1) and its optical properties determined. It was chosen because it was observed to tarnish very rapidly in polished section; although pure, it was not available in large amounts.

In addition to obtaining electron probe analyses of the fresh surfaces of the above-mentioned bornite samples, as shown in Table 1, attempts were made to obtain analyses of the surface region of heavily tarnished material. In spite of using a large beam diameter (defocussed to 50 μm diameter), a low accelerating voltage (15 kV), and a thick carbon coating, all of which would tend to accentuate the contribution of the surface layers to the analysis, significant differences were not detected between tarnished and untarnished bornite using this technique. Clearly the surface tarnish is too thin for compositional differences to be detected using this

TABLE 1. Microprobe analyses of bornite

| | wt% | | | | range wt% | | | |
	Cu	Fe	S	Total	Cu	Fe	S	
BM 31324								
untarnished	62.8	11.4	25.7	99.9	62.6–63.0	11.1–11.6	25.6–25.8	(4 analyses)
tarnished	62.9	11.5	25.8	100.2	62.4–63.2	11.2–11.7	25.4–26.0	(6 analyses)
BM 1969,215								
untarnished	63.6	11.3	25.1	100.0	63.4–63.9	10.9–11.5	24.9–25.3	(4 analyses)
tarnished	63.6	11.3	25.1	100.0	63.4–63.8	10.9–11.6	24.9–25.3	(9 analyses)

Formulae based on four sulphur atoms:

$$BM\ 31324\ Cu_{4.93}Fe_{1.01}S_4$$
$$BM1969,215\ Cu_{5.12}Fe_{1.04}S_4$$

Instrument: Cambridge Instruments Microscan IX

Operating conditions: accelerating voltage: 15kV beam current: 2.50×10^{-8} amps on Faraday cage

Standard: bornite

Emission lines: CuK_α, FeK_α, $S\ K_\alpha$ no other elements detected

method which penetrates 1 μm or more into the sample. However, examination of Table 1 does show the more rapidly tarnishing bornite (BM 1969,215) to have a slight cation excess compared to BM 31324 which is slightly cation deficient. The two samples also differ slightly in Cu : Fe ratio.

Optical properties

The colour changes that result from the atmospheric tarnishing of both fresh fractured surfaces and polished sections of bornite range from brown–orange on a fresh surface through to red–orange, mauve, purple, and finally, to deep blue. These changes can be quantified by spectral reflectance measurements and by the derived colour values.

Measurements were made using a Zeiss Universal microscope with × 16 air and oil objectives and using an SiC standard (Zeiss, 472). The equipment is semi-automated with a step-driven wavelength-scanning line interference filter, S20 Hamamatsu type R938 photomultiplier and a digital voltmeter on-line to a Hewlett Packard programmable calculator. Measurements were made at 10 nm intervals in the range 400 nm to 700 nm. In addition to measurements made in air, three sets of data were obtained in both air and oil (the latter a Zeiss oil, DIN 58.884) allowing calculation of the derived optical constants n and k. Quantitative colour values were calculated relative to the CIE illuminants C and A.

Bornite is pseudotetragonal orthorhombic at room temperature and has a weak but measurable bireflectance of 0.2–0.4% at 400 nm and 0.6–0.7% at 700 nm. Measurements were made on unoriented

grains and R_a, R_b, R_c could not be assigned due to the meagre bireflectance. For the purposes of the experiment, bornite was treated as isotropic, but, in order that direct comparisons could be made, the spectral reflectance scans were obtained with the specimen in exactly the same orientation on the microscope stage. The bireflectance of the tarnished specimens is of the same order as for the untarnished specimens.

Unsmoothed single-run spectral reflectance curves obtained after various periods of tarnishing in air are illustrated in Fig. 1, with the corresponding numerical values listed in Table 2A and the calculated colour values in Table 2B. These show
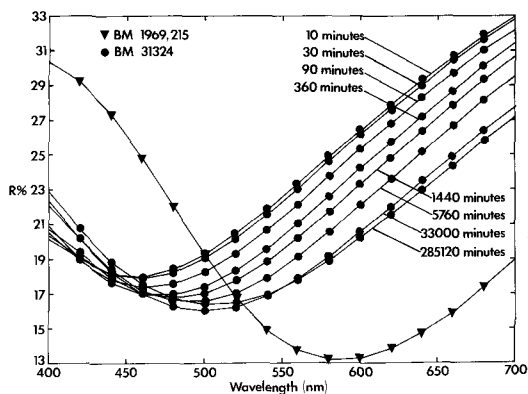

FIG. 1. Spectral reflectance curves in air for bornite specimen BM 31324 showing progressive development of tarnish after exposure to the air, and for the heavily tarnished specimen BM 1969,215.

TABLE 2A. Change in reflectance (R%) of bornite due to tarnishing

Sample BM 31324	wavelength (nm)															
	400	420	440	460	480	500	520	540	560	580	600	620	640	660	680	700
10	20.3	19.1	18.1	18.0	18.4	19.2	20.4	21.8	23.3	24.9	26.4	27.9	29.3	30.6	31.9	32.9
30	20.2	19.1	18.1	17.9	18.2	19.1	20.2	21.6	23.0	24.6	26.2	27.7	29.0	30.4	31.7	32.8
time 90	20.5	19.0	17.8	17.4	17.6	18.3	19.3	20.7	22.1	23.8	25.4	26.8	28.3	29.7	31.1	32.2
(mins) 360	20.9	19.0	17.7	17.0	17.0	17.5	18.3	19.6	21.0	22.6	24.2	25.7	27.2	28.7	30.2	31.4
1440	20.7	19.4	17.9	17.1	16.8	17.1	17.8	18.9	20.2	21.7	23.3	24.9	26.4	27.9	29.3	30.7
5760	22.1	20.2	18.4	17.2	16.6	16.6	17.0	17.9	19.1	20.6	22.1	23.6	25.2	26.6	28.2	29.5
33000	22.4	20.2	18.3	17.0	16.3	16.1	16.3	16.9	17.9	19.1	20.6	22.0	23.5	24.9	26.4	27.8
285120	22.9	20.7	18.8	17.6	16.7	16.4	16.5	17.0	17.8	18.9	20.2	21.6	22.9	24.4	25.8	27.2
Sample BM1969,215 (extreme tarnish)	30.3	29.2	27.3	24.8	22.0	19.3	16.8	14.9	13.7	13.2	13.2	13.8	14.7	15.9	17.4	18.9

TABLE 2B. Change in quantitative colour values of bornite due to tarnishing

Sample BM 31324	C illuminant					A illuminant				
	x	y	λd	Y%	P_e%	x	y	λd	Y%	P_e%
10	.347	.338	585	23.3	15.8	.482	.408	592	24.3	24.2
30	.347	.337	586	23.0	15.5	.482	.408	593	24.1	23.9
90	.347	.335	587	22.2	14.9	.482	.407	594	23.2	23.4
time 360	.346	.331	590	21.1	13.5	.482	.405	595	22.1	21.8
(mins) 1440	.342	.326	594	20.4	11.2	.480	.403	598	21.3	19.2
5760	.337	.319	607	19.5	7.8	.477	.400	604	20.3	15.1
33000	.332	.313	c493	18.3	5.4	.474	.398	616	19.0	11.0
285120	.327	.310	c496	18.3	5.9	.470	.397	648	18.9	8.0
Sample BM 1969,215 (extreme tarnish)	.262	.248	469	15.1	26.0	.406	.372	478	14.5	11.9

that, as observed qualitatively, there is an increase of reflectance with duration of tarnish at 400 nm (the blue end of the visible spectrum) and a decrease in reflectance at 700 nm (the red end of the visible spectrum). This change in reflectance is most marked between 550 nm and 700 nm and a plot of $R\%$ at 600 nm against log time (T) for BM 31324 (Fig. 2) shows an approximate logarithmic relationship except for the first and last measurements which represent, respectively, the onset and retardation of the reaction as an equilibrium position is approached. The spectra shown in Fig. 1 are very similar to those reported by Buckley and Woods (1983) for a cleavage surface of bornite measured in a spectrometer.

One of the problems encountered in this study was the differing tarnishing rates of various bornite samples: BM 31324 would take several years, for example, to reach the degree of tarnish of BM 1969,215 which was acquired in a few months (see Fig. 1). Several factors may affect the rate of tarnish at constant temperature and humidity, among them (i) the associated minerals—qualitative observations on bornite with oriented lamellar inclusions of chalcopyrite coexisting with inclusion-free bornite show that the latter tarnishes more rapidly; (ii) grain size and orientation—granular aggregates with grains in random orientation are observed to tarnish at variable rates, and, in general, the smaller the grain size the slower the tarnish formation; (iii) the nature of the polished surface of the bornite— poorly polished surfaces tarnish more rapidly, due probably to the greater surface area exposed to the atmosphere, and (iv) chemical composition—the data presented in this work show that the cation-deficient bornite tarnished more slowly than that
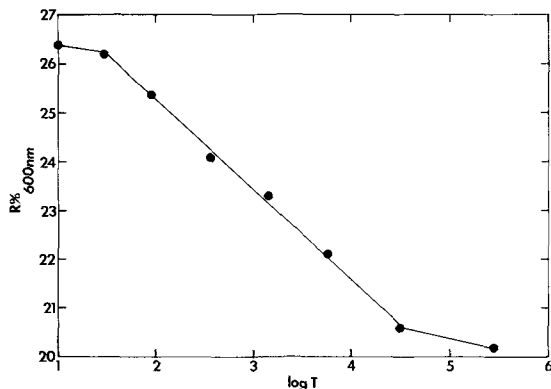
FIG. 2. Plot of reflectance measured at 600 nm wavelength ($R\%$ 600 nm) versus log time (minutes).

with a slight cation excess; many of the so-called 'orange' or 'anomalous' bornites in the literature are cation-deficient (Sillitoe and Clark, 1969; Kosyak, 1969) and their orange appearance may be the result of the retarded tarnishing effect relative to stoichiometric or 'normal' bornite.

Reflectance data obtained in air and in oil for untarnished and tarnished bornite are given in Table 3 and plots of n and k in Figs. 3 and 4. The errors involved in the reflectance measurements are small (of the order of $\pm 0.5\%$ absolute at 400 nm and $\pm 0.2\%$ absolute at 700 nm for single runs). However, as can be seen from Figs. 3 and 4, some of the 400–450 nm n and k values are erroneous.

X-ray photoelectron and Auger electron spectroscopy

X-ray photoelectron spectroscopy (XPS) and Auger electron spectroscopy (AES) have been used previously to study the tarnishing of bornite (Losch and Monhemius, 1976; Buckley and Woods, 1983). In XPS, the kinetic energies of (photo-) electrons ejected when the sample is bombarded with radiation are measured and can be used to obtain directly the binding energies of electrons in core and valence orbitals. In AES, it is not the kinetic energies of these photoelectrons that are measured but the kinetic energies of electrons (the Auger electrons) ejected when the ion resulting from photoemission undergoes relaxation (hence the final state is doubly ionized). The theoretical background and mineralogical applications of both XPS and AES have been reviewed in Berry and Vaughan (1985) and detailed interpretation of the Auger spectra of sulphide minerals discussed by Vaughan and Tossell (1986). For the purposes of this paper, it is sufficient to note that the limited depth of escape of both photoelectrons and Auger electrons makes them powerful techniques for surface analysis. As in other spectroscopic methods, peaks may be assigned to particular elements (and oxidation states) and variations in peak position related to changes in coordination and bonding. Peak intensities may also be used to estimate concentrations; combined with argon ion bombardment (etching) to remove surface layers, variations in concentrations of species with depth beneath the

TABLE 3. Spectral reflectance data for tarnished and untarnished bornites

nm	Untarnished BM 31324 (10 minutes exposure)				Tarnished BM 31324 (285120 minutes exposure)				Extreme tarnish bornite (BM 1969,215)			
	R_{air}	R_{oil}	k	n	R_{air}	R_{oil}	k	n	R_{air}	R_{oil}	k	n
400	20.1	7.3	.57	2.47	22.5	9.3	.78	2.52	30.7	15.6	1.03	3.11
420	18.8	6.6	.59	2.35	20.9	8.0	.66	2.48	29.3	14.6	1.03	2.96
440	17.9	6.3	.65	2.24	19.2	6.9	.59	2.39	27.3	12.8	.80	2.95
460	17.6	6.4	.71	2.16	17.8	6.1	.59	2.27	24.9	10.8	.62	2.84
480	18.0	7.0	.79	2.11	16.9	5.8	.62	2.18	22.2	8.8	.48	2.68
500	18.8	7.8	.87	2.08	16.6	5.8	.67	2.11	19.5	6.9	.41	2.50
520	20.0	8.9	.96	2.07	16.6	6.1	.73	2.05	17.0	5.4	.39	2.33
540	21.3	10.1	1.05	2.07	17.1	6.8	.80	2.00	15.1	4.3	.40	2.18
560	22.9	11.3	1.14	2.09	18.0	7.6	.89	1.97	13.8	3.7	.43	2.07
580	24.4	12.6	1.22	2.10	19.2	8.7	.97	1.96	13.2	3.6	.48	1.99
600	26.0	13.9	1.31	2.14	20.5	9.8	1.05	1.96	13.2	3.9	.56	1.92
620	27.5	15.1	1.38	2.19	21.9	11.0	1.13	1.97	13.6	4.5	.64	1.89
640	28.8	16.3	1.46	2.21	23.3	12.2	1.20	1.97	14.5	5.4	.72	1.86
660	30.2	17.4	1.53	2.26	24.7	13.3	1.27	2.00	15.7	6.4	.81	1.86
680	31.6	18.5	1.59	2.35	26.2	14.5	1.35	2.03	17.1	7.6	.90	1.85
700	32.7	19.5	1.65	2.38	27.5	15.6	1.41	2.07	18.7	8.9	.99	1.86
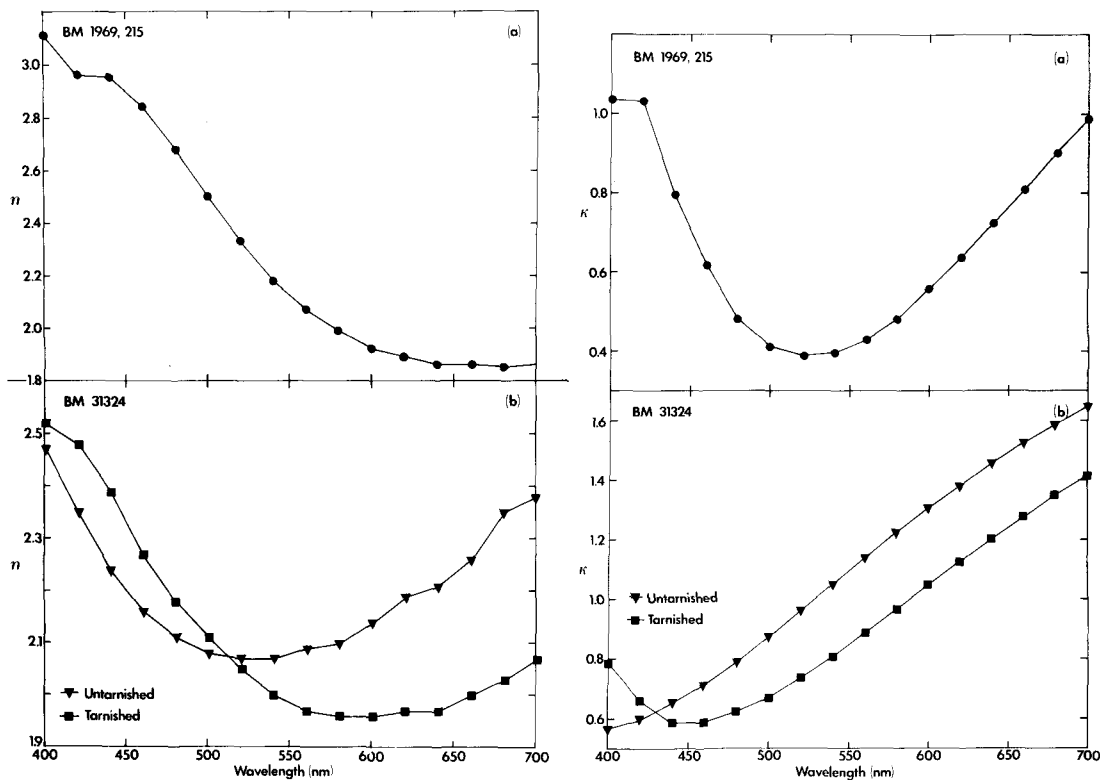
FIGS. 3 and 4. FIG. 3 (*left*). Plot of the optical constant n as a function of wavelength for the heavily tarnished specimen BM 1969,215 and for specimen BM 31324 after 10 mins exposure (untarnished) and 285120 mins exposure (tarnished). FIG. 4 (*right*). Similar plot of the optical constant k as a function of wavelength.

original surface may be measured (depth profiling). In the present work, XPS data were obtained using a Kratos XSAM 800 ESCA-Auger spectrometer with Mg-$K\alpha$ as the exciting radiation. The pressure inside the experimental chamber was $\simeq 10^{-9}$ Torr.

The Fe2p X-ray photoelectron spectra were recorded for the sample in a heavily tarnished state (see Fig. 5a) and show a major peak arising from Fe2$p^{3/2}$ and another peak from Fe2$p^{1/2}$ along with a satellite arising from the presence of Fe^{3+} ions. The maximum of the major peak occurs at 710 eV binding energy with the Fe2$p^{1/2}$ peak at 725 eV and the satellite at 719 eV. The spectrum was again recorded following etching of the sample surface in a stream of argon ions for one minute. The result was a shift in the Fe2$p^{3/2}$ peak to slightly lower binding energy (708 eV) and the virtual disappearance of the Fe^{3+} satellite peak, as shown in Fig. 5b.

These XPS data can be considered in the light of the previous work on bornite by Buckley and Woods (1983) and a systematic study of the core-level electrons in iron oxides undertaken by Mills

and Sullivan (1983). It was noted by Buckley and Woods (1983) that unaltered bornite shows an intensity maximum near 708 eV in the Fe2p spectrum, as found in the present work for the surface after etching. These authors also observed that the intensity maximum for the Fe2p spectrum of the tarnished surface occurs at 711 eV 'consistent with iron being present as an iron (III) oxide'. This is confirmed by the present study and further substantiated by the observation of Fe^{3+} satellites of the type discussed by Mills and Sullivan (1983). As further discussed in the section on conversion electron Mössbauer studies, the oxide present at the surface is almost certainly some form of FeO.OH.

Auger electron spectra were recorded using the same instrument from unetched bornite surfaces, and from surfaces subjected to 5, 15, 45 and 120 minutes etching using argon ions. From the variation in the heights of peaks for S, C, O, Fe, and Cu at kinetic energies of approximately 150, 272, 512, 705, and 920 eV, the relative concentrations of these elements have been estimated as a function of depth
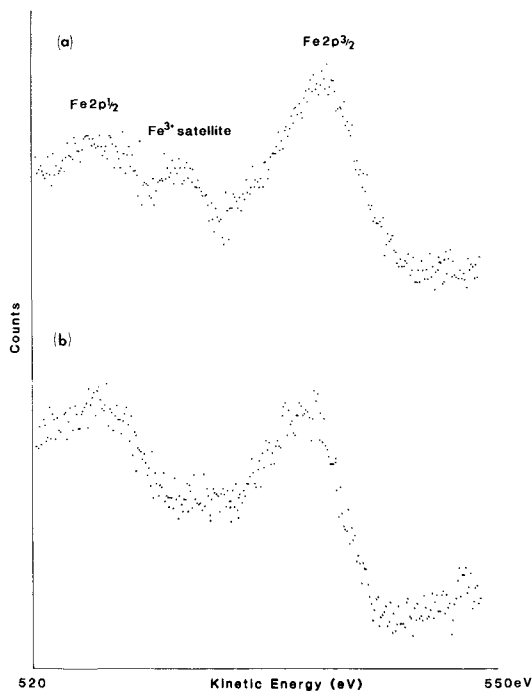
FIG. 5. X-ray photoelectron spectra showing the Fe2*p* peaks for bornite: (*a*) for a heavily tarnished surface; (*b*) the same surface after etching with argon ions for one minute.

ments, the resonant absorption of γ-rays is studied in transmission mode. Conversion electron Mössbauer spectroscopy (CEMS) involves recording the electrons emitted from the sample by processes of internal conversion associated with the decay of nuclei excited by γ-ray absorption. This is a surface-specific technique because of the shallow escape depth of the internally converted electrons (95% originate from within 300 nm of the surface and 60% from within 54 nm). Thus, employing a conventional Mössbauer spectrometer but with a counter to detect electrons emitted from the sample surface, CEMS data can be acquired and provide information on the chemical nature of iron species in the surface region of a sample. Further details of the technique and its applications are given by Tricker (1977, 1981) and by Berry and Vaughan (1985).
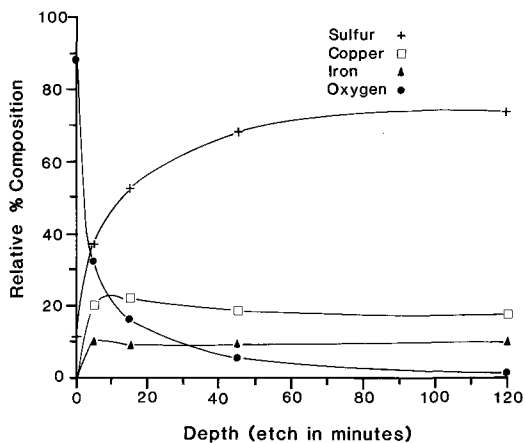

FIG. 6. Relative composition of the surface layers of heavily tarnished bornite as a function of depth obtained from Auger electron spectroscopy.

beneath the surface. The results of this depth profiling Auger study are shown in Fig. 6. A similar study was undertaken by Losch and Monhemius (1976) using synthetic Cu_5FeS_4. The data presented in Fig. 6 show that for heavily tarnished material, very high carbon concentrations are initially observed (due to contamination in the sample chamber) along with relatively high oxygen values. On etching to remove surface layers, a rapid increase in sulphur concentration is observed along with fairly rapid increases in copper and iron. The initial slight increase in oxygen concentration beneath the surface may arise from the removal of the very carbon-rich outer layer to expose the thicker, oxide-rich layer beneath. Qualitatively, the results presented in Fig. 6 resemble very closely those of Losch and Monhemius (1976).

Conversion electron Mössbauer spectroscopy

The Mössbauer effect involving the nucleus of [57]Fe has been widely used in mineralogy to study the oxidation state, spin state, coordination and site distribution of iron in minerals. In these experi-

The conversion electron Mössbauer spectrum of heavily tarnished bornite is shown in Fig. 7, and is interpreted as a single peak with an isomer shift of 0.425 mm/sec relative to iron foil, although it is a broad peak (FWHH = 0.595 mm/sec). These values compare with an isomer shift of 0.39 mm/sec for a doublet with a small quadrupole splitting (0.16 mm/sec) obtained from the transmission spectrum of bornite (see Vaughan and Craig, 1978). The surface spectrum does, therefore, differ from that of the bulk. There is no evidence of the magnetically ordered six-peak spectrum characteristic of well-crystallized hematite or magnetite (one of the species mentioned by Losch and Monhemius,

1976). The observed spectrum could arise from a fine coating of a hydrated ferric oxide, as indicated by some of the other spectroscopic techniques.
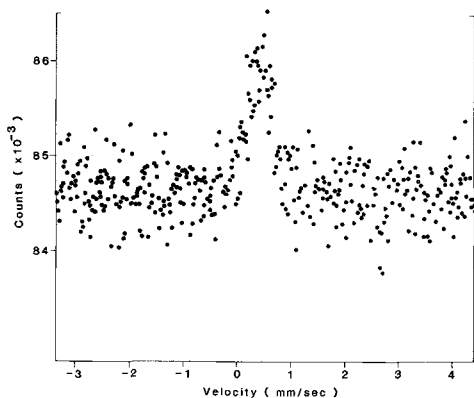

FIG. 7. Conversion electron Mössbauer spectrum of a heavily tarnished bornite surface. The zero of the velocity scale is the centre of gravity of an iron foil spectrum.

Discussion

The crystal structures adopted by the mineral bornite are related to the sphalerite and chalcopyrite structures (which have a cubic close-packed array of sulphur anions with metals in tetrahedral interstices) but only three-quarters of the tetrahedral sites in the anion sublattice are filled. Bornite exists as several polymorphic forms but only the low-temperature form occurs in nature, and was shown by Koto and Morimoto (1975) to be orthorhombic (pseudotetragonal). In the superstructure of low bornite, the metal atoms, although occurring in tetrahedral interstices in the sulphur sublattice, have twelve different coordination types on detailed analysis. However, these can all be considered as either tetrahedrally coordinated or trigonally coordinated; in the latter the metal is sufficiently displaced from the centre of the tetrahedron as to lie nearer the plane of a triangular face.

Although studies have not been undertaken of surface reconstruction in materials as complex as bornite, compounds such as ZnS (sphalerite) have been extensively studied. Work by Duke (1983) and others, based on the results of low-energy electron diffraction (LEED) studies of semiconductors, shows that in compounds such as ZnS, displacements of the cation and anion from their bulk positions by $\simeq 0.5$ Å occur in the uppermost layer. Thus, on the (110) surface of ZnS, for which both Zn and S are three-coordinate, a reconstruction occurs with a movement of Zn atoms inward (towards the

bulk) and of the S atoms outward. Harrison (1976, 1980) has explained these changes in terms of a conversion of half-occupied dangling bond hybrid orbitals at both Zn and S on the unreconstructed surface to a combination of a fully occupied bond orbital on S and an unoccupied orbital on Zn for the reconstructed surface. The reconstruction stabilizes the orbital at S and converts it from sp^3 to s in type, while the Zn orbital is destabilized and converted from sp^3 to sp^2. An equivalent description within the delocalized molecular orbital approach and employing s and p orbitals only would relate the three-coordinate Zn site to a six valence electron AB_3 species, expected to be planar as in BH_3, and the three-coordinate S site to an eight valence electron AB_3 species, expected to be pyramidal as in NH_3 (Burdett, 1980; Tossell, 1984). The degree of distortion will be dependent on the change in energy of the surface orbital upon distortion in the angle $B-A-B$. This will depend partly upon the difference in electronegativity between the cation and anion involved, with a smaller electronegativity difference giving a larger degree of distortion from the unreconstructed geometry. Thus, for example, experiment shows that ZnS suffers a larger reconstruction than ZnO. Since Cu and Fe are of similar electronegativity to Zn, we anticipate that the CuS_3 and FeS_3 groups on the surface of bornite will all be distorted towards a planar coordination.

The question then arises as to how these distortions may affect the Zn and Fe 3d orbital energies in the surface region. Calculations using the multiple scattering Xα (MS-Xα) method have previously been undertaken on polyhedral units representative of the copper and iron sulphides and used to model their electronic structures in bulk (see, for example, Tossell, 1978; Vaughan and Tossell, 1980, 1983). Thus, calculations on Cu^{+1} in tetrahedral and triangular planar coordination with sulphur (on CuS_4^{-7} and CuS_3^{-5} clusters) show that Cu^{+1} is stable in triangular coordination; the bonding is considerably more covalent, with the lowest binding energy orbitals (of Cu3d–S3p bonding character) slightly stabilized relative to a tetrahedral environment (Tossell, 1978). Although calculations have been performed on a cluster representing tetrahedrally coordinated Fe^{3+} (i.e. the FeS_4^{-5} cluster), calculations have not been performed for an Fe^{3+} ion in planar triangular coordination. However, trigonal planar Fe^{3+} is apparently not found in sulphide minerals, suggesting its instability.

The evidence presented in this paper and by previous workers suggests that the rapid oxidation of the bornite surface produces a hydrated iron (Fe^{3+}) oxide. This, in turn, raises the question of

what other changes occur in surface composition, particularly as regards the copper and sulphur species. The XPS work of Buckley and Woods (1983) indicates a copper sulphide layer (suggested to be initially of composition Cu_5S_4) immediately beneath the iron hydroxide. Evidence was also presented by these authors for the presence of Cu^{2+} produced by further oxidation of the Cu_5S_4 and this species may also be associated with surface areas exhibiting a distinctly blue tarnish, although colour differences may also result from differences in thickness of the oxidized layer (Holloway et al., 1982). Buckley and Woods (1983) also noted the tendency for minor Ag in bornite to become concentrated in the tarnish layer where it is present in the copper sulphide oxidation product.

Although the spectral range studied in the reflectance measurements is very limited, tentative conclusions can be drawn by comparison with spectroscopic studies of sulphides and oxides and the results of calculations on relevant systems. The reflectance spectra $(R\%)$ of untarnished and tarnished bornite (Fig. 1) illustrate the shift of the minimum between two peaks (one in the ultraviolet and one in the infra-red region of the spectrum) from 460 nm (untarnished) to 500 nm (tarnished) to 590 nm (extreme tarnish). Plots of the constants n and k (Figs. 3 and 4) against wavelength show a similar trend with the development of a 'peak' towards the high energy end of the range (400 nm) with increasing tarnish; there is a corresponding reduction in n and k towards the red end of the spectrum (700 nm).

Comparison of the reflectance spectra of the extreme tarnish bornite with the diffuse reflectance spectra for sulphides and oxides (Wood and Strens, 1979; Strens and Wood, 1979), taken with the results of calculations on the electronic structures of iron-oxygen cluster units representative of Fe^{2+} and Fe^{3+} sites in oxide and hydroxide minerals (Tossell et al., 1974), suggests that the peak which develops at high energy could arise from $Fe^{3+} \rightarrow O$ charge transfer. The agreement is best when this feature is compared with the peaks observed in the diffuse reflectance spectra of the FeO.OH polymorphs (Strens and Wood, 1979) which are in marked contrast to the diffuse reflectance spectra of (presumably untarnished) bornite (Wood and Strens, 1979). However, the reflectance data and the derived n and k values for the extreme tarnish bornite are also close to those (taking an average of R_o and R_e) for one of the blue-remaining covellines, yarrowite (Criddle and Stanley, 1986-QDF 2.418) which has a formula close to Cu_5S_4. It is therefore possible that the formation of a Cu_5S_4 layer gives rise to the significant optical changes during bornite tarnishing described in this paper.

The surface oxidation of bornite and the products of this reaction may result from the surface reconstruction, leading to Cu^{+1} and Fe^{+3} in coordination approximating trigonal planar, and the relative destabilization of the Fe^{+3} in this environment. The iron would undergo reaction to form the hydrated oxide in which Fe^{3+} is stable in octahedral coordination, leaving the copper in its more favoured trigonal coordination in the underlying sulphide layer. Silver, which also favours a 3-fold coordination (Vaughan and Craig, 1978), would be concentrated in the copper sulphide layer. Similar processes would be expected at the surfaces of other Cu–Fe sulphides containing the metals in tetrahedral coordination. Indeed, XPS studies of the oxidation of chalcopyrite (Buckley and Woods, 1984) also show concentration of iron at the surface to form a hydroxy-oxide with concomitant formation of a copper sulphide. The more rapid rate of tarnish in bornite may be a consequence of more rapid diffusion of iron towards the surface in a structure containing more vacant tetrahedral sites. Further studies of the Cu–Fe sulphides involving low-energy electron diffraction, calculations and spectroscopic work are in progress to test these models.

References

Berry, F. J. and Vaughan, D. J. (1985) *Chemical Bonding and Spectroscopy in Mineral Chemistry.* Chapman and Hall, London.
Buckley, A. N. and Woods, R. (1983) *Austral. J. Chem.* **36**, 1793–804.
——(1984) Ibid. **37**, 2403–13.
Burdett, J. K. (1980) *Molecular Shapes: Theoretical models of Inorganic Stereochemistry.* Wiley-Interscience, New York.
Criddle, A. J. and Stanley, C. J. (1986) *The Quantitative Data File for Ore Minerals.* British Museum (Natural History) 455 pp.
Duke, C. B. (1983) *J. Vac. Sci. Technol.* **B1**(3), 732–5.
Harrison, W. (1976) *Surface Sci.* **55**, 234.
——(1980) *Electronic Structure and the Properties of Solids.* W. H. Freeman and Co.
Holloway, P. H., Remond, G. and Schwartz, W. E. Jr (1982) In *Interfacial Phenomena in Mineral Processing* (B. Yarrar and D. J. Spottiswood, eds.) Engineering Foundation, New York.

Kosyak, Y. A. (1969) *Dokl. Akad. Nauk SSSR,* **186,** 921–3.

Koto, K. and Morimoto, N. (1975) *Acta Crystallogr.* **B31,** 2268–73.

Losch, W. and Monhemius, A. J. (1976) *Surface Sci.* **60,** 196–210.

Mills, P. and Sullivan, J. L. (1983) *J. Phys. D: Appl. Phys.* **16,** 723–32.

Sillitoe, R. H. and Clark, A. H. (1969) *Am. Mineral.* **54,** 1684–710.

Strens, R. G. J. and Wood, B. J. (1979) *Mineral. Mag.* **43,** 347–54.

Tossell, J. A. (1978) *Phys. Chem. Minerals* **2,** 225–36.

——(1984) Ibid. **11,** 81–4.

——Vaughan, D. J. and Johnson, K. H. (1974) *Am. Mineral.* **59,** 319–34.

Tricker, M. (1977) In *Surface and Defect Properties of Solids,* Vol. 6 (M. W. Roberts and J. H. Thomas, eds.). The Chemical Society, London.

——(1981) In *Mössbauer Spectroscopy and its Chemical Applications* (J. G. Stevens and G. Sheney, eds.). Adv. in Chem. Series, Am. Chem. Soc., Washington.

Vaughan, D. J. and Craig, J. R. (1978) *Mineral Chemistry of Metal Sulfides,* Cambridge Univ. Press.

——and Tossell, J. A. (1980) *Can. Mineral.* **18,** 157–63.

————(1983) *Phys. Chem. Minerals* **9,** 253–62.

————(1986) Ibid. **13,** 347–50.

Wood, B. J. and Strens, R. G. J. (1979) *Mineral. Mag.* **43,** 509–18.